NUREG/CR-5847
ORNL/Sub/79-7778/8

The Influence of Precompression on the Lower-Bound Initiation Toughness of A 533 B Reactor-Grade Steel

Prepared by
J. W. Dally, G. R. Irwin, X-J. Zhang, R. J. Bonenberger

Department of Mechanical Engineering
University of Maryland

Oak Ridge National Laboratory

Prepared for
U.S. Nuclear Regulatory Commission

AVAILABILITY NOTICE

Availability of Reference Materials Cited in NRC Publications

Most documents cited in NRC publications will be available from one of the following sources:

1. The NRC Public Document Room, 2120 L Street, NW., Lower Level, Washington, DC 20555

2. The Superintendent of Documents, U.S. Government Printing Office, P.O. Box 37082, Washington, DC 20013-7082

3. The National Technical Information Service, Springfield, VA 22161

Although the listing that follows represents the majority of documents cited in NRC publications, it is not intended to be exhaustive.

Referenced documents available for inspection and copying for a fee from the NRC Public Document Room include NRC correspondence and internal NRC memoranda; NRC bulletins, circulars, information notices, inspection and investigation notices; licensee event reports; vendor reports and correspondence; Commission papers; and applicant and licensee documents and correspondence.

The following documents in the NUREG series are available for purchase from the GPO Sales Program: formal NRC staff and contractor reports, NRC-sponsored conference proceedings, international agreement reports, grant publications, and NRC booklets and brochures. Also available are regulatory guides, NRC regulations in the *Code of Federal Regulations*, and *Nuclear Regulatory Commission Issuances*.

Documents available from the National Technical Information Service include NUREG-series reports and technical reports prepared by other Federal agencies and reports prepared by the Atomic Energy Commission, forerunner agency to the Nuclear Regulatory Commission.

Documents available from public and special technical libraries include all open literature items, such as books, journal articles, and transactions. *Federal Register* notices, Federal and State legislation, and congressional reports can usually be obtained from these libraries.

Documents such as theses, dissertations, foreign reports and translations, and non-NRC conference proceedings are available for purchase from the organization sponsoring the publication cited.

Single copies of NRC draft reports are available free, to the extent of supply, upon written request to the Office of Administration, Distribution and Mail Services Section, U.S. Nuclear Regulatory Commission, Washington, DC 20555.

Copies of industry codes and standards used in a substantive manner in the NRC regulatory process are maintained at the NRC Library, 7920 Norfolk Avenue, Bethesda, Maryland, for use by the public. Codes and standards are usually copyrighted and may be purchased from the originating organization or, if they are American National Standards, from the American National Standards Institute, 1430 Broadway, New York, NY 10018.

NUREG/CR-5847
ORNL/Sub/79-7778/8
RF

The Influence of Precompression on the Lower-Bound Initiation Toughness of A 533 B Reactor-Grade Steel

Manuscript Completed: April 1992
Date Published: May 1992

Prepared by
J. W. Dally, G. R. Irwin, X-J. Zhang, R. J. Bonenberger

Department of Mechanical Engineering
University of Maryland
College Park, MD 20742

Under Contract to:
Oak Ridge National Laboratory
Operated by Martin Marietta Energy Systems, Inc.

Oak Ridge National Laboratory
Oak Ridge, TN 37831-6285

Prepared for
Division of Engineering
Office of Nuclear Regulatory Research
U.S. Nuclear Regulatory Commission
Washington, DC 20555
NRC FIN B0119
Under Contract No. DE-AC05-84OR21400

Abstract

The lower-bound initiation toughness of two different heats of A 533 B reactor-grade steel was determined over temperatures in the brittle-to-ductile transition region. The lower-bound toughness was measured by depressing the initiation toughness with dynamic loading, high constraint offered by notched round bars, and axial precompression of the material in the fracture process zone.

This report first describes the test method employing a precompressed round bar subjected to impact loading to initiate a cleavage fracture. The procedure to convert strain measurement into dynamic initiation toughness K_{Id} is described. Also, the results of a fractographic analysis are correlated with the features observed on the strain-time traces, and techniques used to distinguish initiation by either cleavage or ductile tearing are presented.

The effect of the amount of precompression on cleavage initiation and K_{Id} was examined at two temperatures, $T^* = 43$ and 65°C. It was determined that the amount of precompression required to initiate cleavage increased with temperature T^*. It was observed that increasing precompression deformation increased the probability of, but did not ensure, cleavage initiation. Although the number of tests were limited, the amount of precompression deformation appeared to influence K_{Id} results. Specifically, a range of precompression for each test temperature seemed to produce successful cleavage initiations and valid K_{Id} determinations. Insufficient or excessive amounts of precompression gave incorrect K_{Id} measurements. At these relatively high temperatures, the A 533 B steel exhibits significant ductility, and it was observed that K_{Id} associated with initiation by cleavage or by ductile tearing was nearly the same.

Contents

List of Figures

List of Tables

Nomenclature

a = radius of the notched section (mm)
a_e = effective radius of the notched section (mm)
b = radius of the shoulder section (mm)
d = diameter of the notched section (mm)
D = diameter of the shoulder section (mm)
E = Young's modulus of elasticity (MPa)
$F_3\ (a_e/b)$ = a numerical function
K or K_I = opening mode stress-intensity factor ($MPa\cdot\sqrt{m}$)
K_{Ia} = crack-arrest toughness ($MPa\cdot\sqrt{m}$)
K_{Ic} = static initiation toughness ($MPa\cdot\sqrt{m}$)
K_{Id} = dynamic initiation toughness ($MPa\cdot\sqrt{m}$)
K_{IR} = lower-bound initiation toughness ($MPa\cdot\sqrt{m}$)
r_Y = exclusion adjustment for residual stress effects (mm)
RT_{NDT} = reference nil-ductility temperature (°C)
T = test temperature (°C)
T^* = difference between test temperature and RT_{NDT} (°C)
δ = axial deformation due to precompression (mm)
ε_0 = gross section strain (m/m)
ε_{max} = maximum strain (m/m)
σ_0 = gross section stress (MPa)
σ_n = net section stress (MPa)
σ_Y = plastic flow stress (MPa)

1 Introduction

Crack-arrest toughness K_{Ia} indicates the stress intensity K below which fine-scale cleavage events, even when initiated, are unable to spread and join, thus representing a lower-bound toughness. However, the current understanding of cleavage-fibrous behavior for nuclear reactor vessel steels suggests that a method of cleavage initiation testing with small specimens may provide the same lower-bound data for toughness with more efficiency. The large amount of scatter observed in the test results[1–3] handicaps slow-load, small-specimen testing to determine cleavage initiation toughness. This large scatter indicates that cleavage initiation along the crack front in a small specimen must be considered as a rare event. Only when the number of small specimen tests is large do the lowest observed values correspond with the toughness determinations from large specimens with long crack fronts. However, the probability for cleavage initiation is enhanced by notch embrittlement, rapid loading, and constraint. Lower-bound determinations of initiation toughness reported here are based on the failure of the cleavage sites to initiate, spread, and join. Recently, Dally et al.[4] have developed a testing procedure that uses relatively small specimens for determining the lower-bound initiation toughness of A 508 reactor-grade steel. The results show much less scatter than slow-load testing methods; this is a valuable attribute relative to the number of specimens needed to obtain valid lower-bound toughness values.

This report presents rapid-load measurements of the cleavage initiation toughness of A 533 B reactor-grade steel over a limited range of temperatures near the brittle-to-ductile transition region. The approach described in Ref. 4 was used in this series of measurements. A critical element in the success of small-specimen determination of the lower-bound cleavage initiation toughness is to increase the severity of the local stresses adjacent to the precrack. By increasing the stresses local to the crack front and using plastic deformation of the material in the neighborhood of the crack tip, it is possible to more nearly match the probability of cleavage initiation sites that occur in large specimens or in components with a long crack front.

The specimen used in this study is a circumferentially notched round bar that provides significant constraint with a large elevation of the flow stress. Impact loading also serves to elevate the flow stress due to strain rate effects. Finally, a circular precrack, concentric with the round bar, is formed by axial compression. The axial compression, which produces yielding and plastic flow at the notched section, closes a small segment at the root of the notch to form a pseudo crack, as indicated in Fig. 1. Upon release of the compression load, a small natural crack is formed at the tip of this pseudo crack. The precompression process also produces residual tensile stresses at the crack tip; this further elevates the stress to increase severity of the local stress state and enhance the probability of a lower-bound cleavage initiation.

This report describes in detail the method of applying the impact load to the specimen. Also described is the method of precompression and the influence of the amount of this precompression. Strain-time traces are included to characterize the response of the specimen to the impact loading. A method is presented to determine if the initiation was valid. A method for interpreting the strain-time traces to give the dynamic initiation toughness K_{Id}, corresponding to the lower-bound toughness K_{IR}, is shown. An interpretation of the fracture behavior of the specimen based on the strain-time response is given. The results of a fractographic analysis are presented and correlated with the behavior observed from the strain-time traces. Finally, the results from this study are compared with the crack-arrest toughness K_{Ia} of the same material, established through independent programs that involved extensive testing.

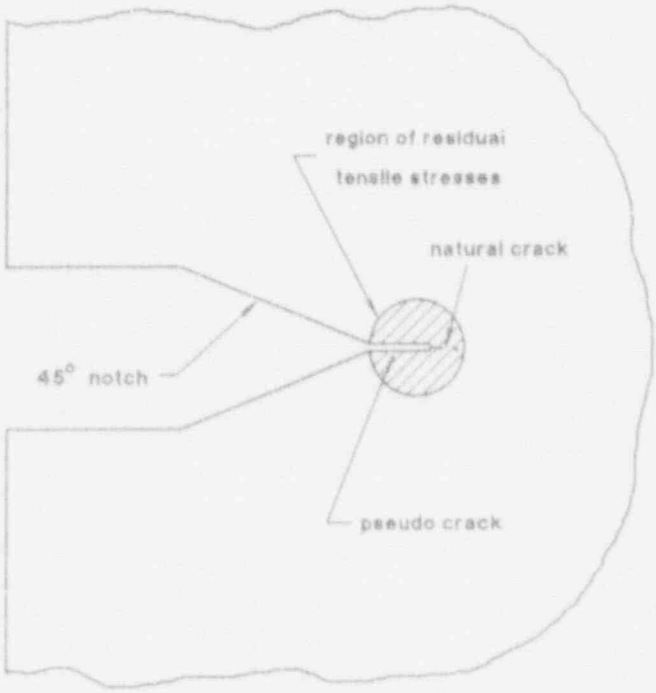

Figure 1 Axial precompression load yields notched region of bar and forms pseudo crack. Upon unloading, a natural crack develops in region of residual tensile stress

2 Notched Round-Bar Specimen

The purpose of using a notched round bar in a dynamic fracture-initiation experiment is to simulate, with a relatively small diameter bar, the constraint provided by a very thick, plate-type fracture specimen. A rigorous comparison of constraint afforded by a plate specimen of thickness B and a notched round bar with a shoulder diameter D has not been established; however, it is believed that the constraint provided by a notched round bar is at least equivalent to that provided in central regions of a plate specimen with a thickness equal to π times the net-section diameter d.*

The round-bar specimens used in this initial study are illustrated in Fig. 2. In both geometries, the nominal shoulder

*This estimate assumes the thickness of a plate specimen (B) is equivalent to the net-section circumference of the round bar, giving the relation, $B = \pi d$.

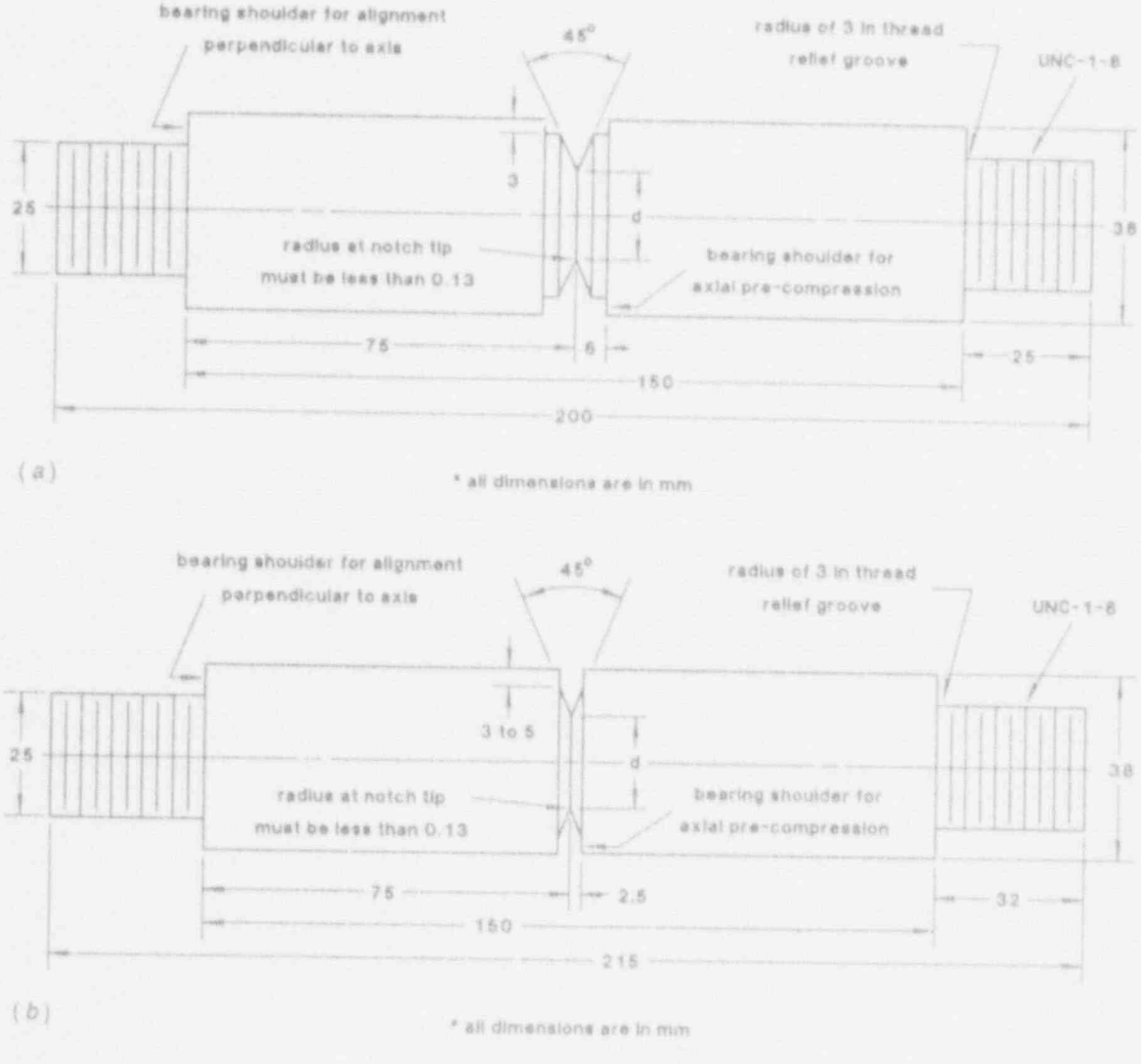

Figure 2 (*a*) Original round-bar specimen with cut-away bearing shoulder, and (*b*) modified round-bar specimen. Net diameter d is a variable ranging from 13 to 19 mm

diameter D is 38 mm, and the diameter d defining the notch section varied from 13 to 19 mm. The notch was machined with a 45° included angle, using a tool with a tip radius r = 0.13 mm. The specimen was shouldered at each end to provide accurately machined bearing surfaces perpendicular to the specimen axis. These bearing surfaces were essential to ensure alignment of the specimen in the impact loading device. Both ends of the bar were threaded (1-8 UNC) to provide a means for attaching the specimen to the loading train.

The total length of the bar was 200 to 215 mm, with 150 mm used for the center section. This section accommodated the notch while providing a uniform cross-sectional area of length L = 2D above and below the notch. Shoulders located in line with the notch are used to measure and control the amount of permanent, axial deformation imposed on the notch during the initial precompression. Strain gages were mounted at a distance D above and below the notch to measure the nominal strains imposed on the specimen during impact loading.

3 Tensile Impact Loading Tower

The essential features of the loading tower are shown in Fig. 3, where the delivery end of the system is illustrated. The impact load is developed by dropping a weight of 59 kg from a height that is adjustable from 0 to 1.8 m. The weight is fitted at its upper end with a brass bushing and at its lower end with a hardened steel insert (AISI 4340 with Rockwell C scale hardness R_C = 48). The bushing and insert both serve as bearings and keep the weight in alignment with the center rod.

The center rod is fabricated from 50-mm-diam drill stock and fitted with an internal 1-8 UNC thread at its lower end. This rod supports the top end of the round-bar specimen. A load transmission tube fits over the round-bar specimen overlapping the center rod by 25 mm. An anvil, threaded onto the other end of the specimen, supports the load transmission tube. All of the contacting surfaces on the loading fixture, namely, the weight insert, transmission tube, and anvil, are flat and square to the axis of the center rod to ensure axial impact. These surfaces are hardened to limit localized surface yielding; this facilitates a high loading rate.

The weight delivery system is supported by a four-column frame. Heavy steel plates 50 mm thick serve as the top and bottom platens. The center rod extends through the top platen. The top end of the center rod is threaded so that it can be positioned vertically with two hex nuts located on each side of the top platen.

The impact velocity of the weight with the maximum drop distance is 6 m/s. The energy delivered to the load transmission tube is 1053 N-m. However, the loading rate and the stress in the specimen depend mainly on the impact velocity rather than the available drop-weight energy. In addition, the stresses and the load rate depend on the geometry of the specimen and the yield characteristics of the material being tested. The load imposed on the notched round bar is measured directly during the impact period with strain gages that are mounted on the test specimen.

4 Axial Precompression of Notch

While the tip of the notch was machined with a radius r of about 0.13 mm, the sharpness of the notch tip is much less than that of a fatigue precrack. Moreover, with tough steels, fracture did not initiate during impact with the maximum available drop-weight velocity and r = 0.13 mm. Previous studies conducted by Mylonas[5,6] and Turner[7,8] showed that initiation of cleavage fractures in mild steels could be assisted by application of a compressive load to a notched specimen, thus producing plastic deformation and residual tension in the notch region. When the specimen is subsequently loaded in tension, cleavage initiation might occur after an extremely short extension of the crack tip by ductile hole joining. Following this concept, the notches on the specimens were sharpened before testing by applying an axial compressive load that exceeded the uniaxial yield strength of A 533 B steel (483 MPa) by a significant factor. Yielding at the notched section of the bar caused the sides of the notch near the tip to move together to produce a pseudo crack as shown in Fig. 1.

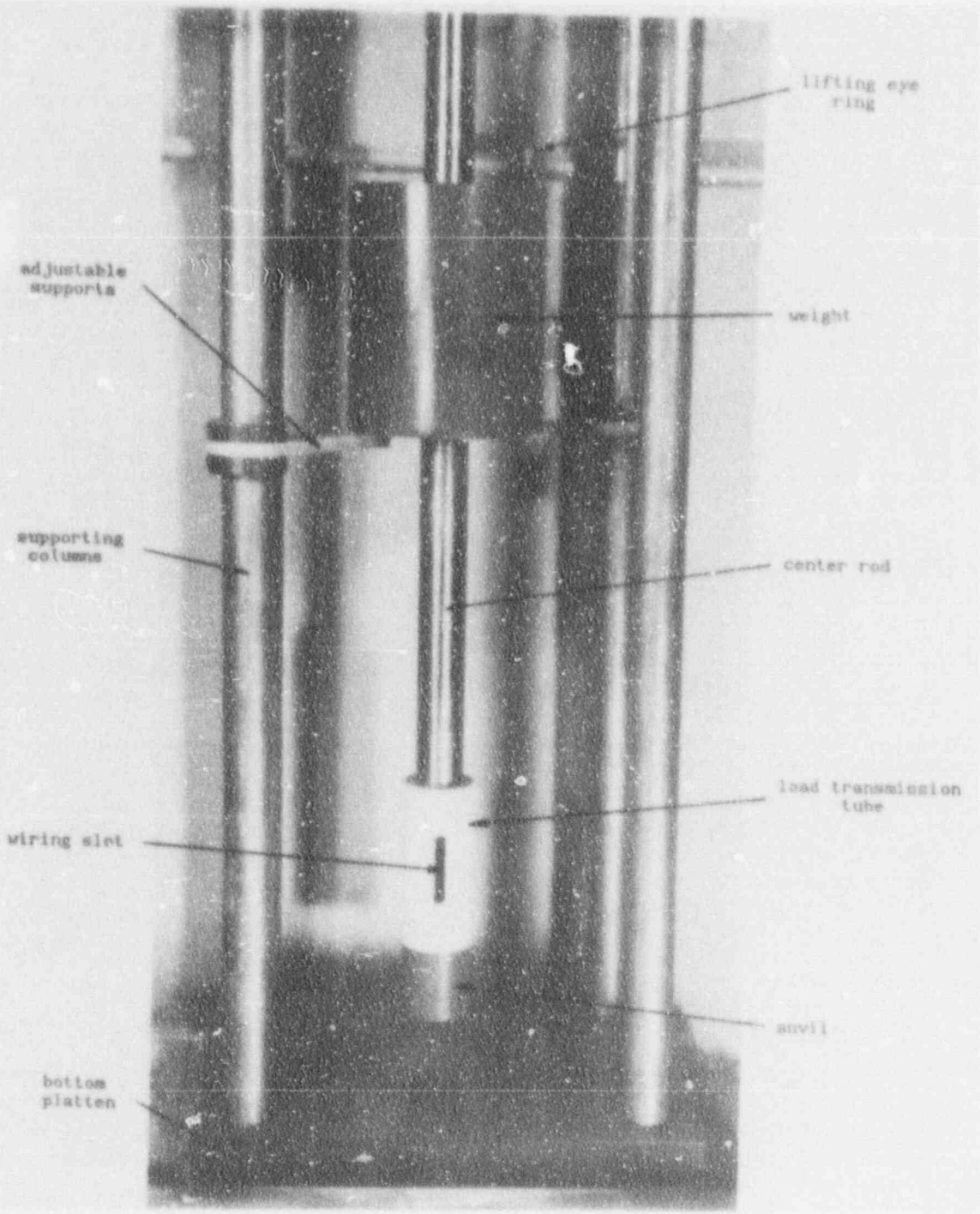

Figure 3 Features at delivery end of tensile-impact-loading device

The straight crack shown in Fig. 1 is the pseudo crack formed by closing the two sides of the notch as the region local to the notch and, to a lesser degree, the central region both yield. A short crack extension occurs at a shallow angle to the pseudo crack. This extension is a natural crack produced by the residual tensile stresses that develop as the axial load is removed from the bar.

The effect of the precompression process on the mechanical properties of the steel is not known. Under the axial compression load, the material very close to the notch root is strained plastically to levels in the range of 10 to 20%. With this large amount of plastic strain, some degree of work hardening could be expected; however, the Bauschinger effect mitigates this increase. Because the round bar is preloaded in compression and then tested in tension, the Bauschinger effect should produce a reduction in the tensile yield strength and an apparent softening of the material close to the notch. It is believed that the change in mechanical properties are small because the work hardening of these low-carbon steels at these strain levels is not large and the hardening and Bauschinger effects tend to cancel each other.

In using this method of crack sharpening, it is important that the compression of the notch be uniform about the circumference. To facilitate uniform deformation, the round bar was fitted with end anvils with their bearing surfaces perpendicular to the axis of the bar. Also, a split V-groove fixture was clamped to the body of the bar to prevent any off-axis bending of the bar by the compressive load. The uniformity achieved is demonstrated in a 5.5× fractograph (Fig. 4), where the pseudo crack appears as a ring with a uniform thickness.

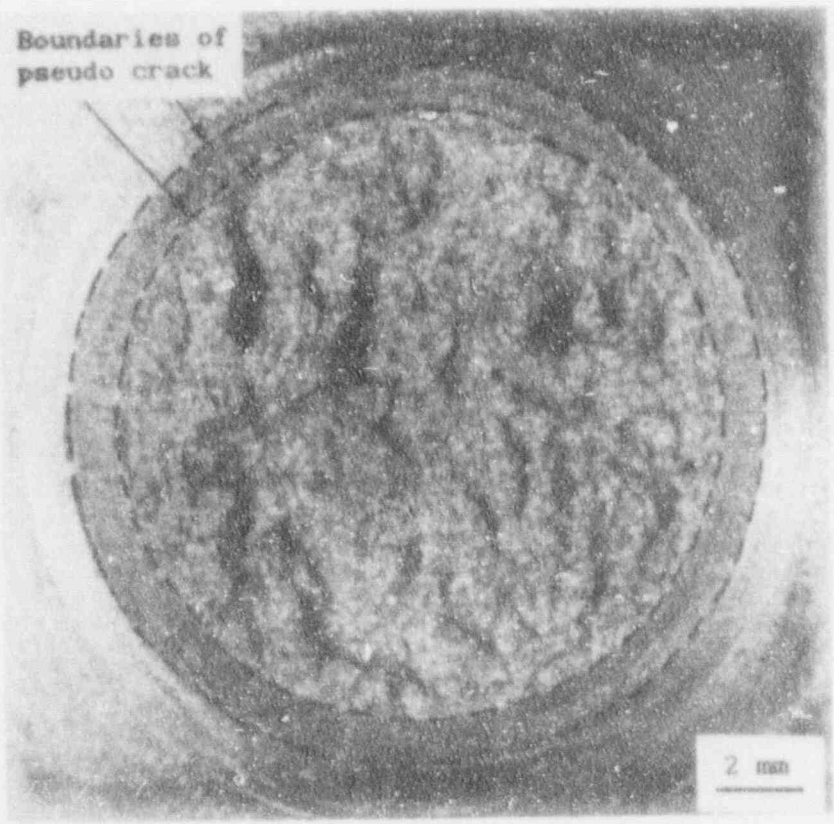

Figure 4 Fracture surface showing uniform depth of pseudo crack about circumference

Axial

In addition to the control of the deformation of the notched section about the circumference, it is also necessary to control the amount of axial compression. Sufficient axial deformation must occur to sharpen the notch tip and to induce large residual tensile stresses at the root of the notch. To better control the axial deformation, steel spacing rings of a suitable thickness were placed in the notch area shoulders (Fig. 5). The rings acted as mechanical stops, controlling the axial deformation so that it was uniform around the circumference. By using several rings with varying heights, different amounts of deformation were imposed.

The compression load required to produce the axial deformation was measured directly on the universal testing machine that was used in precompressing the round bars.

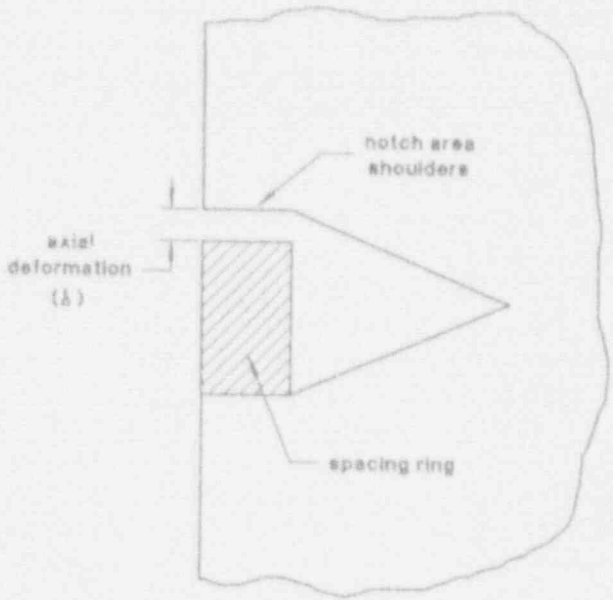

Figure 5 Split spacing rings for controlling plastic deformation imposed during precompression

5 Test Procedure

Six strain gages were employed to determine the load imposed on the notched round-bar specimens during impact. The gages were oriented in the axial direction and placed at 120° intervals around the specimen at a distance of 1D above and below the notch. The gages exhibited a nominal resistance of 350 Ω and a gage length of 1.6 mm. The individual gages were connected to a Wheatstone bridge/amplifier unit, capable of 100 kHz, for appropriate signal conditioning.

A type J, iron-constantan thermocouple with a resolution of 0.1°C was adhesively bonded in the notch to measure the test temperature of the specimen. The specimens were tested over a range of temperatures from 3 to 60°C. When the test temperature differed from room temperature, dry ice was used to cool the specimens, and a resistance heater attached to the bottom anvil was used to heat the specimens.

All of the tests were conducted using the maximum capacity of the loading frame, with a drop of 1.8 m for the weight. As the weight strikes the transmission tube, a compressive stress wave propagates through the tube and into the anvil. Upon encountering the bottom free surface of the anvil, the compressive pulse is reflected as a tensile pulse and propagates upward into the notched-bar specimen. As expected, the strain gages mounted below the notch responded first, and the gages mounted above the notch responded about 15 μs later. This lag is due to the time required for the tensile stress wave, propagating at about 5 mm/μs, to travel the distance between the gage sets. The loading of the specimen increases monotonically at a rate on the order of 10/s in the shoulder section. Of course, the strain rate in the notched section is higher due to the reduced cross-sectional area and the strain concentration effect of the notch. It is believed that the strain rate exceeds 500/s* at the notch tip. The symmetry among the gages in each set is very good, indicating a uniform axial loading of the specimen.†

The voltage output from one of the bottom strain gages was used to initiate the sweep of three dual-channel, digital storage oscilloscopes to ensure that the voltage-time trace for each gage was recorded on a common time base. The

*Five percent strain in 100 μs.

†An example of the symmetry in the strain-time traces is shown in Ref. 4.

analog-to-digital converter on each of the oscilloscopes was set to sample at a rate of 200 ns/point. After the test, the voltage-time traces were downloaded from the oscilloscope memories to a personal computer for further data processing.

6 Lower-Bound Fracture-Initiation Toughness

The method of analysis to determine the dynamic initiation toughness K_{Id} from strain-time traces recorded from the round bar during impact testing is based on relations derived for static loading. For a notched, round bar subjected to uniaxial tension, the stress-intensity factor is given by Tada et al.[9] as

$$K_I = \sigma_n \sqrt{\pi b}\, F_3(a_e/b) \quad , \tag{1}$$

where F (a /b) is a function defined by

$$F_3(a_e/b) = (1/2)\sqrt{(a_e/b)\left[1-(a_e/b)\right]}\left[1 + 0.5(a_e/b) + 0.375(a_e/b)^2 - 0.363(a_e/b)^3 + 0.731(a_e/b)^4\right] \quad . \tag{2}$$

Note also that

$$\sigma_n = (b/a_e)^2 \sigma_0 \quad . \tag{3}$$

The effective radius a_e of the net section is given by

$$a_e = a - r_Y \quad , \tag{4}$$

where r_Y is an exclusion adjustment to account for the effect of residual stress at the tip of the pseudo crack. The adjustment r_Y is expressed as

$$r_Y = (1/2\pi)(K/\sigma_Y)^2 \quad . \tag{5}$$

In determining r_Y, the plastic flow stress σ_Y, allowing for constraint and rapid loading, was assumed to be 1091 MPa, and K was the estimate of the stress-intensity factor before the adjustment of the radius of the net section. Note that r_Y is not determined in an iterative manner because only the initial estimate of K is substituted into Eq. (5).

The flow stress was determined by first increasing the static yield strength of A 533 B steel by a factor of 1.87 from 483 to 905 MPa to account for the constraint. Next, strain-rate effects were considered by adding another 186 MPa, a common practice for structural steels. These adjustments for constraint and strain-rate effects gave a dynamic, plastic flow stress estimate of 1091 MPa.

For uniaxial loading, the strain measured on the shoulder section of the bar is

$$\varepsilon_0 = \sigma_0/E \quad , \tag{6}$$

where E is 207 GPa for carbon steel. If the strain ε_0 in Eq. (6) is the strain measured at initiation (ε_{max}), then application of Eqs. (1) through (5) gives the dynamic initiation toughness K_{Id}.

The difference between the static and dynamic solutions for the stress-intensity factor K and the J-integral for notched round bars has been analyzed with finite elements by Nakamura, Shih, and Freund.[10] The dynamic loading was a tension pulse that increased linearly with time for a 50-μs period. Nakamura et al. found that the J-integral resulting from the tension pulse was essentially the same as that produced by static loading of the same magnitude. The referenced study was performed to justify the data analysis method used by Costin, Duffy, and Freund[11] in determining K_{Id} and J_{Id} from data taken with Hopkinson bar experiments. Because the round-bar experiments described here involve nominal strain rates two to three times lower than the strain rates produced in a Hopkinson bar, it is evident that the static analysis described above is adequate for predicting the dynamic initiation toughness K_{Id} from the strain data from the notched round bar.

7 Test Results

Two series of tests were performed in this program to determine the lower-bound initiation toughness of A 533 B reactor-grade steel. In the first series, 20 notched round bars were fabricated from heat No. 1 of the A 533 B steel that exhibited a reference nil-ductility temperature of RT_{NDT} = -2°C. These specimens were tested with axial impact loading at temperatures ranging from 3 to 60°C. The objective of this first series of tests was to determine K_{Id} as a function of temperature in the brittle-to-ductile transition region.

In the second series, 12 notched round bars were fabricated from A 533 B reactor-grade steel; however, these came from a different heat of steel. At the time of testing, it was not known that the material had been changed from heat No. 1 to heat No. 2. It was apparent only in the analysis of the data that the materials were found to be different. Indeed, the RT_{NDT} = –23°C for heat No. 2, was significantly different. The objective of this second series of tests was to examine the effect of the amount of axial precompression on the K_{Id} measurements.

7.1 Results from Test Series No. 1—A 533 B Heat No. 1

Twenty specimens fabricated from heat No. 1 were tested in axial impact over a range of temperatures from 3 to 60°C. Of this group, 11 specimens failed in a manner such that a valid (acceptable) K_{Id} could be determined. The voltage-time data for each strain gage were converted to give six strain-time traces for each specimen tested. From a preliminary observation of these traces, the failure behavior could be determined. The round-bar specimens failed either by (1) cleavage with very small amounts of ductile tearing or (2) extensive ductile tearing before cleavage initiation. The type of behavior with limited tearing yields data that permit a valid value of K_{Id} to be determined from Eqs. (1) to (6). If the tearing is extensive, however, K_{Id} cannot be measured, and the test is not valid. Examples of strain-time traces from valid and invalid tests are shown in Figs. 6 and 7, respectively. For a valid test, the strain-time trace exhibits a single peak value that marks the failure of the specimen. The strain increases monotonically with time for about 100 to 140 μs after the stress wave reaches a bottom gage, and then the load decreases rapidly after failure initiates. For an invalid test, a typical strain-time trace is shown in Fig. 7. The high-level strain is maintained for an extended period of time, partial unloading/reloading takes place in the specimen, and complete failure does not occur for 500 μs or more. These observations of the characteristic features on the strain-time traces allow separation of the

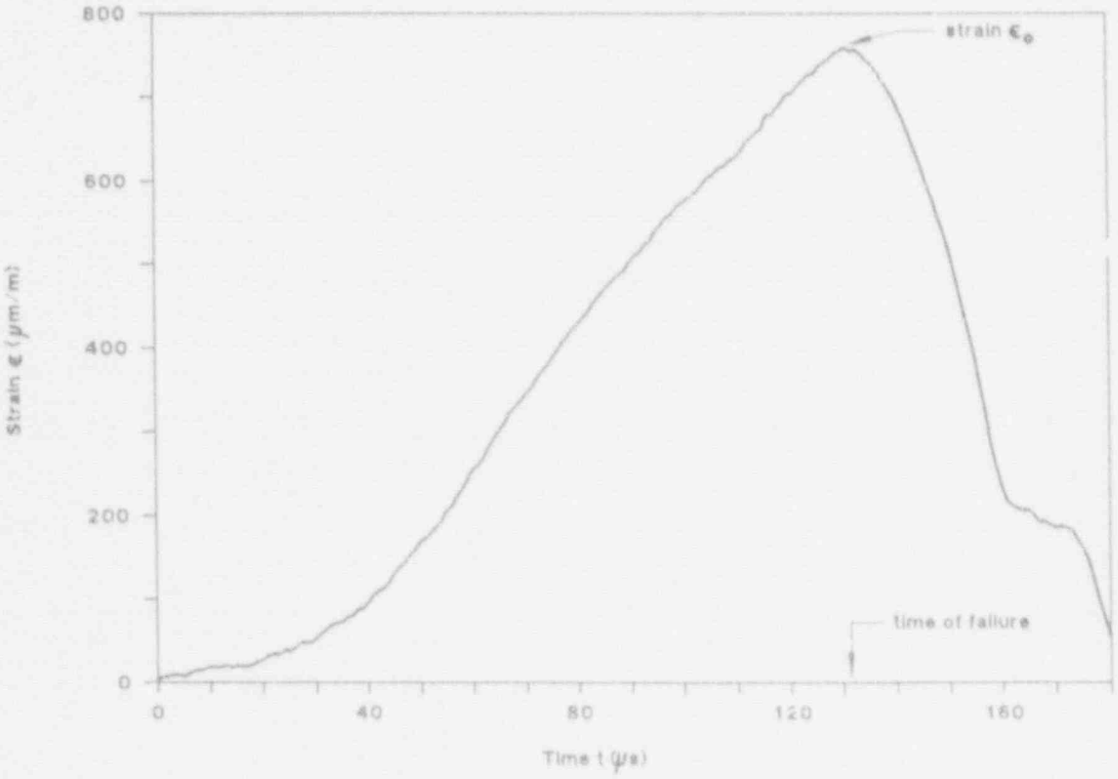

Figure 6 Strain-time trace associated with valid test (gage-average trace)

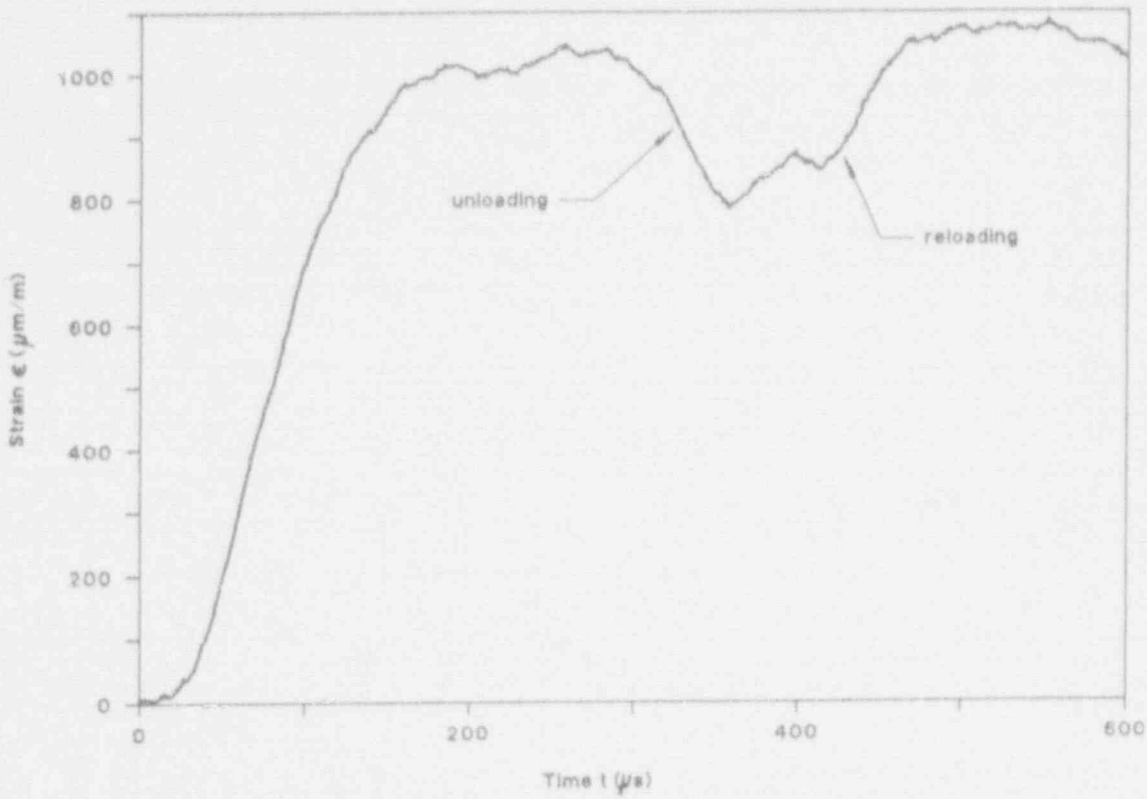

Figure 7 Strain-time trace associated with invalid test (gage-average trace)

specimens failing by brittle cleavage from those failing by excessive ductile tearing before cleavage initiation.

Several common features are observed in all of the strain-time traces that yield valid K_{Id} values (Fig. 8). Three traces are shown: (1) the average of all three bottom gages, (2) the average of all three top gages, and (3) the average of all six gages. It is clear that the bottom gages initially respond before the top gages because of the delay due to the time required for the stress wave to travel between the gage sets. Both sets of gages initially increase monotonically, with the bottom gages registering higher strains than the top gages. This initial part of the loading process is dominated by stress-wave behavior. At ~95 μs, after the stress wave reaches the lower gages, the strain-time traces cross over, and the top gages indicate strains slightly higher than the bottom gages. It is believed that the crossover is due to stress-wave reflection from the notch discontinuity, which suppresses the strain on the lower gages. After the crossover point, the traces from both gage sets correspond closely with the average of all six gages until failure at 120 μs. This close correspondence indicates that stress-wave effects have diminished and that a quasi-static loading is prevalent. Both traces record simultaneously the strain at failure, which is the highest point on each trace. The simultaneity is expected because the notch is centrally located between the gages, and the time for the unloading waves to reach the bottom and top gages is equal. For the time period between crossover and failure, the two different averages give the nominal strain ε_0 with deviations of ±9%.

The maximum strain determined from the strain-time traces was used as the failure strain ε_{max} for the 11 qualifying tests. Values of K_{Id} were calculated for each of the six strains recorded. Two averaging methods were then used to determine a total K_{Id} for each specimen. First, the peak values ε_{max} from the six individual strain-time traces were averaged to compute K_{Id}. Second, all of the strain-time traces were averaged into a single trace, and K_{Id} was computed from the peak value of this combined trace. The difference in K_{Id} between these methods was only 4%, demonstrating the equivalency of both procedures. All subsequent K_{Id} values presented were determined by using the first method. The results for K_{Id}, which approximates

Test

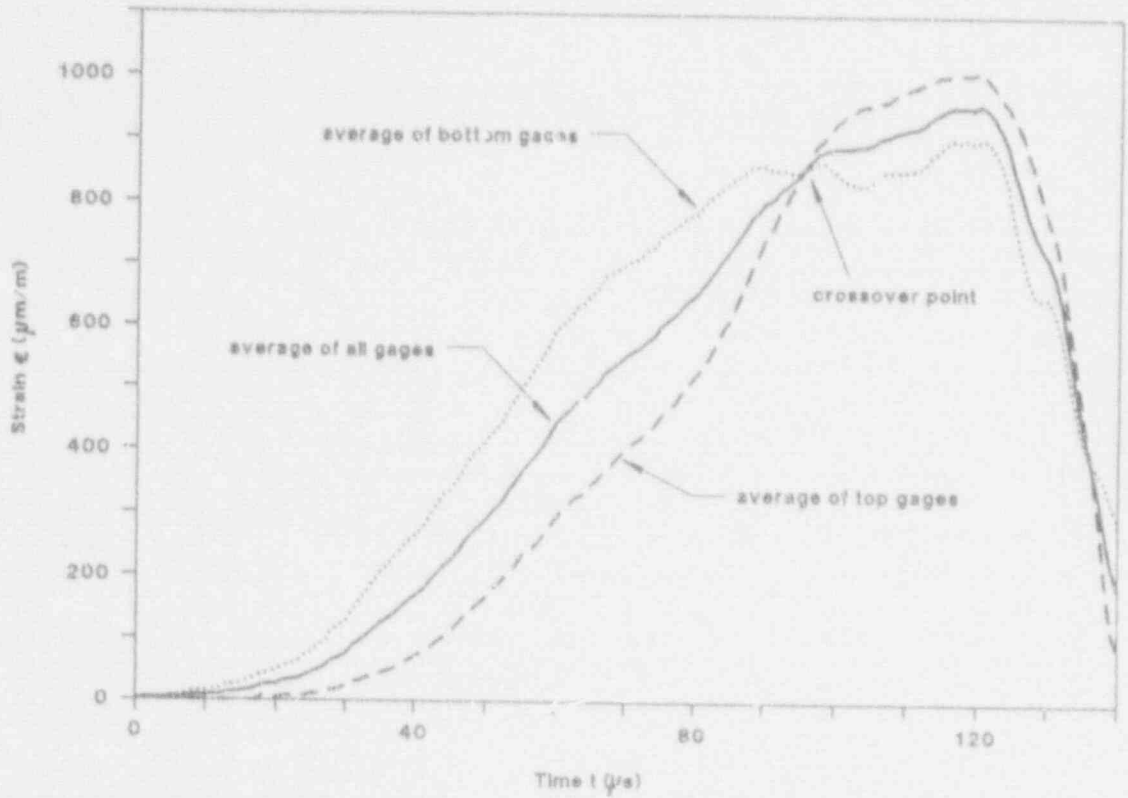

Figure 8 Typical features observed on strain-time traces associated with valid impact fractures

the lower-bound initiation toughness, are shown as a function of temperature in Fig. 9.

Examination of Fig. 9 shows that K_{Id} varied from 74 to 116 MPa•$\sqrt{m}$ as the temperature $T^* = (T - RT_{NDT})$ increased from 5 to 52°C. There is a clear trend for the initiation toughness to increase with temperature; however, the scatter in the data, particularly at the higher temperatures, prevents one from quantifying this trend. The results from all 20 of the notched round bars tested in this first series of experiments are listed in Table 1.

At relatively low temperatures, T* ranging from 5 to 11°C, all three tests (B-5, B-6, and B-8) were valid, and the results for K_{Id} were tightly clustered, as shown in Fig. 9. Also, valid determinations could be achieved with d = 19 mm. As the temperature T* was increased to midrange in this series (22 to 34°C), valid initiation was more difficult to achieve. Of the ten specimens tested (B-1, B-2, B-4, B-5, B-7, C-2, C-5, C-8, C-9, and C-11), only four provided valid data for determining K_{Id}. It was necessary (except for specimen B-1) to decrease d from 19 to 15.2 mm to increase the strain at the notch and promote valid initiations. The precompression was also increased with T* in an attempt to increase the number of initiation sites available to trigger cleavage at the higher temperatures. Note from Fig. 9 that the degree of scatter increased.

For the highest temperatures with T* in the range from 44 to 52°C, valid results were achieved in four of the six experiments conducted (C-1, C-3, C-4, C-6, C-7, and C-12). The high rate of success was partly fortuitous, but decreasing the notched diameter to 15.2 mm and increasing the amount of precompression at the higher temperatures enhanced the probability of cleavage initiation. Again the scatter in these four data points was moderate (±10%).

One test (C-10) was conducted at T* = 62°C; however, the specimen exhibited appreciable ductile tearing before cleavage initiation and, accordingly, did not provide data for a valid K_{Id} determination. It may be possible to measure a lower-bound K_{Id} at T* = 62°C or above if the neck diameter of the round bar is decreased to 12.7 mm and if the precompression is increased. Unfortunately, sufficient

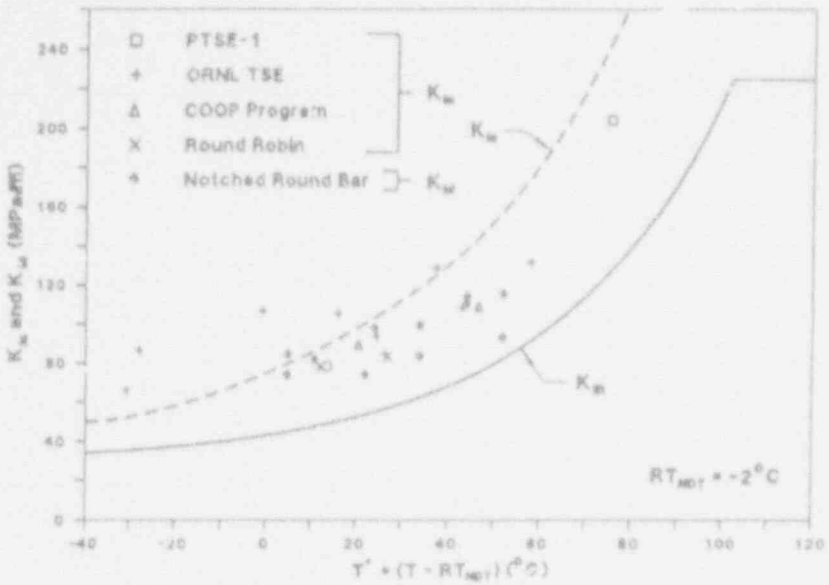

Figure 9 Lower-bound initiation toughness as function of temperature T* for A 533 B reactor-grade steel, heat No. 1 with RT_{NDT} = –2°C

Table 1 Summary of results for the first test series of A 533 B reactor-grade steel with RT_{NDT} = –2°C

Test ID	K_{Id} (MPa•$\sqrt{m}$)	δ (mm)	T (°C)	T* (°C)	d (mm)	Test validity
B-1	93.7	*a*	22.2	24.2	19.0	Yes
B-2	95.3	0.406	26.1	28.1	19.0	No
B-3	73.9	0.406	2.8	4.8	19.0	Yes
B-4	100.7	0.381	26.1	28.1	19.0	No
B-5	94.8	0.432	28.3	30.3	19.0	No
B-6	82.0	0.381	8.9	10.9	19.0	Yes
B-7	96.9	0.432	28.3	30.3	19.0	No
B-8	84.5	0.406	2.9	4.9	19.0	Yes
C-1	116.0	0.940	50.1	52.1	15.2	Yes
C-2	52.5	2.210	20.0	22.0	15.2	No[b]
C-3	150.0	0.965	50.0	52.0	15.2	No
C-4	110.7	0.432	42.0	44.0	15.2	Yes
C-5	74.2	0.483	20.0	22.0	15.2	Yes
C-6	166.0	0.457	49.7	51.7	15.2	No
C-7	114.4	0.483	32.1	44.1	15.2	Yes
C-8	145.9	0.508	32.0	34.0	12.7	No
C-9	83.8	0.533	62.0	34.0	12.7	Yes
C-10	133.5	1.245	60.0	62.0	15.2	No
C-11	99.8	1.118	32.0	34.0	15.2	Yes
C-12	93.9	1.194	50.0	52.0	15.2	Yes

[a]Not determined.
[b]Cleavage was initiated, but damage due to precompression was excessive.

specimens were not available to establish the feasibility of testing at or above $T^* = 62°C$.

In Fig. 9, the results from the notched round bar are also compared with the crack-arrest toughness K_{Ia} for the same material determined in other test programs including pressurized-thermal-shock experiments (PTSEs), ORNL thermal-shock experiments (ORNL TSEs), the COOP program, and the Round Robin program.[12] It is evident that the results from the notched round bar compare closely with the determinations made in these other programs. The largest differences were with the results from the ORNL TSE. While there was very good agreement with the data from PTSE-1, the COOP program, and the Round Robin experiments, the toughness measured with the round bar was usually lower than that determined with TSE.

Note also that in all instances the lower bound of the notched round-bar measurements exceeded the ASME minimum toughness curve K_{IR}.

7.2 Results from Test Series No. 2—A 533 B Heat No. 2

After completing test series No. 1, questions were raised regarding the amount of precompression required to initiate cleavage with a minimum of crack extension by ductile hole joining. In the first series, the axial deformation imposed was varied, and it was noted that increasing the deformation aided in introducing cleavage initiation sites and improved the probability of obtaining valid data for K_{Id} determination of the lower-bound toughness. However, the functional relation of the amount of precompression δ or K_{Id} was not known at any of the test temperatures.

To investigate the effect of precompression, it was planned to test six notched round-bar specimens at $T^* = 22°C$ and another six specimens at $T^* = 44°C$. The amount of precompression was to be increased systematically, and K_{Id} was to be measured during the impact experiments. This plan was based on experience developed during the first test series, where steel from heat No. 1 with $RT_{NDT} = -2°C$ often exhibited cleavage initiation when the amount of precompression $\delta = 0.5$ mm at test temperatures was in the range from 20 to 42°C. It was not known that the specimens for test series No. 2 were from a different heat of A 533 B steel with $RT_{NDT} = -23°C$. This fact was learned only after the second test series was complete, while attempts were being made to explain the significant discrepancies between the results for K_{Id} from the two series of experiments. The results obtained in the second test series are given in Table 2.

The first six bars, with a notch diameter d = 19 mm, were tested at T = 20°C, equivalent to $T^* = 43°C$. Three bars (D-2a, D-5a, and D-6a) with precompressions δ = 0.356, 0.711, and 0.838 mm initiated in cleavage at K_{Id} = 79.2, 78.6, and 84.3 MPa$\sqrt{m}$, respectively. The other three bars (D-1a, D-3a, and D-4a) with precompressions δ of 0.229, 0.483, and 0.610 mm did not initiate in cleavage. Indeed, these three specimens did not fail even by ductile hole joining and remained intact during the impact test.

It was decided to retest bars D-1, D-3, and D-4. Initially, all three bars were precompressed again (D-1b, D-3b, andD-4b), imposing δ = 0.889, 1.118, and 1.321 mm in the second cycle. Bar D-1b was retested but again remained intact during impact. The notch diameter was then reduced from 19 to 15.2 mm, a third cycle of precompression with δ = 0.813 mm was applied (D-1c), and the bar was retested for the third time. Cleavage was initiated in this attempt, giving K_{Id} = 95.0 MPa$\sqrt{m}$.

The notch diameter of bars D-3 and D-4 were then reduced to 15.2 mm, and large precompressions of δ = 1.346 and 1.092 mm were applied (third cycle). These bars (D-3c and D-4c) failed in cleavage at artificially low values of K_{Id}. Observations of the strain-time traces indicated that failure occurred before the crossover point (Fig. 8), while the loading was dominated by stress wave effects. The combination of low K_{Id} and failure before crossover implies excessive damage from precompression.

An examination of the results in Table 2 shows a general trend on the effect of the amount of precompression. For the six specimens with d = 19 mm that were subjected to one cycle of precompression, only one of the four round bars with $\delta < 0.7$ mm failed in cleavage. However, valid K_{Id} values were obtained for both specimens with $\delta >$ 0.7 mm. For the three specimens with d = 15.2 mm that experienced multiple precompression cycles, cleavage successfully initiated in all of the specimens. However, the strain-time traces for the specimens with $\delta > 0.9$ mm indicated failure in <80 μs and at artificially low K_{Id} levels. Such behavior suggests that the material in the notched

Table 2 Summary of results for the second test series of A 533 B reactor-grade steel with $RT_{NDT} = -23°C$

Test ID	K_{Id} (MPa·√m)	δ (mm)	T (°C)	T* (°C)	d (mm)	Number of cycles	Test validity
D-1a	77.0	0.229	20.0	43.0	19.0	1	No
D-2a	79.2	0.356	20.0	43.0	19.0	1	Yes
D-3a	75.7	0.483	20.0	43.0	19.0	1	No
D-4a	57.3	0.610	20.0	43.0	19.0	1	No
D-5a	78.6	0.711	20.0	43.0	19.0	1	Yes
D-6a	84.3	0.838	20.0	43.0	19.0	1	Yes
D-1b	102.2	0.889	20.0	43.0	19.0	2	No
D-3b[a]		1.118			19.0	2	
D-4b[a]		1.321			19.0	2	
D-1c	95.0	0.813	20.0	43.0	15.2	3	Yes
D-4c	78.1	1.092	20.0	43.0	15.2	3	No[b]
D-3c	58.2	1.346	20.0	43.0	15.2	3	No[b]
E-2a	118.0	0.229	42.0	65.0	15.2	1	No
E-1a	124.1	0.381	42.0	65.0	15.2	1	No
E-3a	116.8	0.483	42.0	65.0	15.2	1	No
E-6a	125.1	0.914	42.2	65.2	15.2	1	No
E-4a	127.5	1.397	42.0	65.0	15.2	1	No
E-5a	126.0	1.549	42.0	65.0	15.2	1	No
E-2b	125.4	1.372	42.1	65.1	15.2	2	No
E-5b	117.0	1.524	42.0	65.0	15.2	2	Yes
E-4b	129.7	1.600	42.0	65.0	15.2	2	Yes
E-6b	99.0	1.778	42.0	65.0	15.2	2	No[b]

[a]Specimen was precompressed but not tested.
[b]Cleavage was initiated, but damage due to precompression was excessive.

region had been damaged by excessive amounts of precompression. Therefore, it appears that precompressions δ in the range 0.7 to 0.9 mm are necessary to reliably initiate cleavage in round bars with notch diameters between 15.2 and 19 mm at T = 20°C.

The limited data obtained in this test series indicate that the amount of precompression is important in introducing cleavage sites near the tip of the pseudo crack, but the number of cycles of precompression does not appear to affect the initiation toughness K_{Id} in any systematic manner. The data supporting this observation are shown in Table 3.

The scatter in K_{Id} associated with the valid tests, where cleavage was initiated very early in the fracture process, was relatively small. Deviations from the average value of $K_{Id} = 84.3$ MPa·√m ranged from -6.8 to +12.7%.

In four tests at 20°C (D-1a, D-3a, D-4a, and D-1b) the round bar did not fail during impact. The round bars accommodated the input energy by yielding either at the notch or in the threads used to attach the bars to the loading fixture. In three instances (D-1a, D-3a, and D-4a), yielding (probably at the threads) limited K_I to less than $(K_{Id})_{Ave}$. In these cases, sufficient stress was not imposed on the bar to induce failure either by tearing or by cleavage initiation.

Reducing the notch diameter from 19 to 15.2 mm elevates the stress in the notched region and produces failure of the specimens at T = 20°C. However, failure of specimens D-3c and D-4c was by cleavage initiation at fairly low K_{Id}

Table 3 Summary of valid test results for heat No. 2 of A 533 B steel tested at T = 20°C ($T^* = 43$°C)

Test ID	d (mm)	δ (mm)	Number of cycles	K_{Id} (MPa•$\sqrt{m}$)	Deviation (%)
D-2a	19.0	0.356	1	79.2	-6.0
D-5a	19.0	0.711	1	78.6	-6.8
D-6a	19.0	0.838	1	84.3	0.0
D-1c	15.2	0.813	3	95.0	+12.0
			$(K_{Id})_{Ave}$ =	84.3	

levels (58.2 and 78.1 MPa•$\sqrt{m}$, respectively), which is attributed to an excessive amount of precompression.

In the second group of six specimens tested at 42°C (E-1a to E-6a), no failures by cleavage occurred. Indeed, four specimens did not fail and remained intact during the impact loading. Specimens E-1a and E-3a failed by initiation by ductile hole joining at K_{Id} = 124.1 and 116.8 MPa•$\sqrt{m}$, respectively. The four specimens that did not fail were precompressed a second time with increased δ and tested again. Two of these specimens (E-5b and E-4b) failed with cleavage initiation at K_{Id} = 117.0 and 129.7 MPa•$\sqrt{m}$, respectively. One of the remaining specimens (E-2b) failed with initiation by ductile hole joining at K_{Id} = 125.4 MPa•$\sqrt{m}$. The final specimen (E-6b) failed prematurely in cleavage at 99.0 MPa•$\sqrt{m}$.

The data from the six failures at T = 42°C are summarized in Table 4. Inspection of these results shows that the initiation toughness in cleavage and in tearing by ductile hole joining is approximately the same at this test temperature. The amount of precompression δ appears to affect the initiation toughness. Specifically, a precompression in the range from 1.5 to 1.6 mm seems necessary to reliably trigger cleavage fracture for round bars with d = 15.2 mm at T = 42°C. Precompressions δ < 1.5 mm do not impose sufficient damage to induce cleavage initiation, and precompressions δ > 1.6 mm cause too much damage in the notched region.

The results for K_{Id} associated with cleavage failure for heat No. 2 are shown in Fig. 10. The range of the temperature T^* for these results is from 43 to 65°C, which is well into the transition region. All six of the values for K_{Id} fall above the K_{IR} line and below the K_{Ia} line. Three of the four points plotted along T^* = 43°C appear low when compared to the results for heat No. 1. However, both of the data points for T^* = 65°C compare favorably with the results from heat No. 1 and with ORNL thermal-shock tests.

Table 4 Summary of results for heat No. 2 of A 533 B steel tested at T = 42°C (T^* = 65°C)

Initiation mode	Test ID	δ (mm)	K_{Id} (MPa•$\sqrt{m}$)	$(K_{Id})_{Ave}$ (MPa•$\sqrt{m}$)
DHJ[a]	E-1a	0.381	124.1	122.1
DHJ	E-3a	0.483	116.8	122.1
DHJ	E-2b	1.372	125.4	122.1
Cleavage	E-5b	1.524	117.0	123.4
Cleavage	E-4b	1.600	129.7	123.4
Cleavage[b]	E-6b	1.778	99.0	

[a]DHJ means "ductile hole joining."
[b]Cleavage was initiated, but damage due to precompression was excessive.

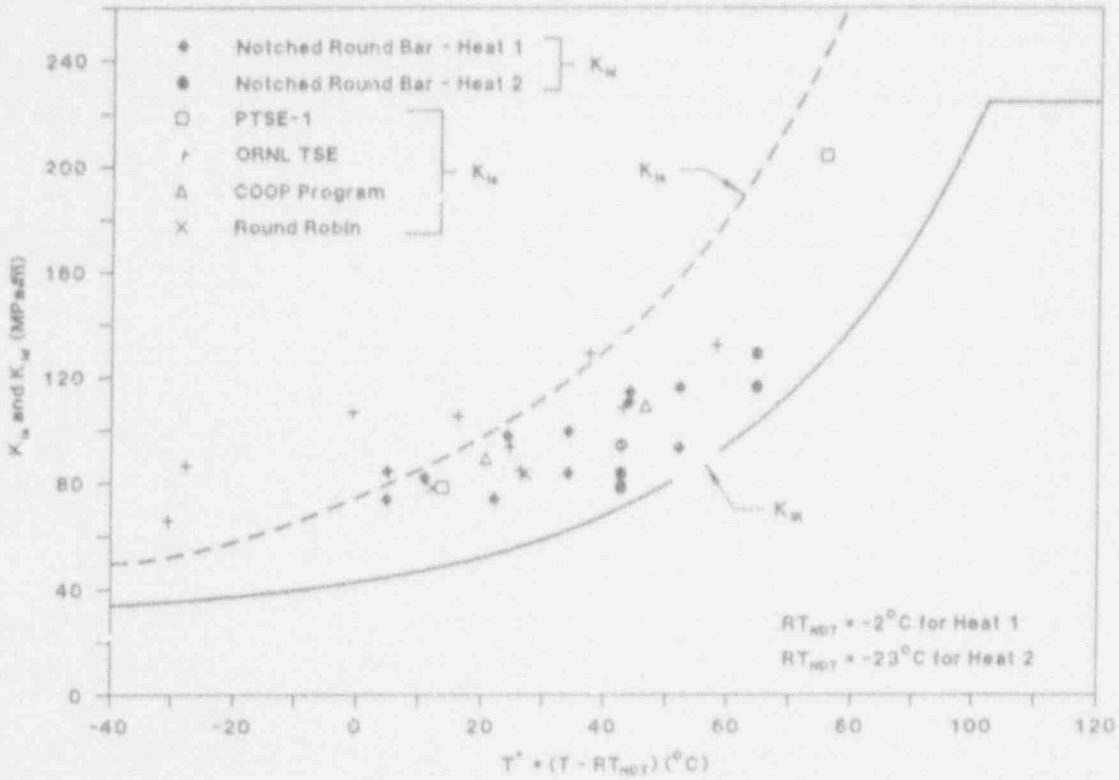

Figure 10 Lower-bound initiation toughness as function of temperature T* for A 533 B steel, heat Nos. 1 and 2

8 Discussion

The results showing K_{Id} as a function of the amount of precompression for heat No. 2 are summarized in Figs. 11 and 12. The results from the tests at T = 20°C (T* = 43°C) (Fig. 11) show that the amount of precompression seems to influence K_{Id}. Precompression is necessary to initiate cleavage, and the probability of initiating cleavage increases with the amount of precompression. When the amount of precompression imposed is not of sufficient magnitude, the specimen is able to absorb the impact energy, and cleavage is not initiated. Also, when the amount of imposed precompression is excessive, the material in the notched region is severely damaged, and cleavage initiates at artificially low stress levels. Between these two extremes lies a range of precompression that gives reliable cleavage initiations and suitable toughness determinations. For this heat of A 533 B steel (RT_{NDT} = -23°C) at the testing temperature (T = 20°C), the appropriate precompression deformation δ is from 0.7 to 0.9 mm.

The results for the tests at T = 42°C (T* = 65°C) (Fig. 12) illustrate similar effects, except that the amount of precompression required to initiate cleavage is much higher. A minimum precompression of δ = 1.5 mm was required before initiation sites were produced that could be activated with a dynamically applied K_I of ~120 MPa$\sqrt{m}$. Also, the upper bound of appropriate precompression seems to be 1.6 mm for this testing temperature. Clearly, the increase in the test temperature has elevated the initiation toughness for both cleavage initiation and for tearing initiation. The velocity of the crack front extending by ductile hole joining was measured at 0.50 and 3.93 m/s in specimens where the crack advanced by 0.52 and 1.42 mm, respectively.

Finally, as the temperature T* increases, it becomes more difficult to initiate cleavage, as failure by tearing becomes the predominant mode of failure. Cleavage initiation can be induced at a temperature T* of 65°C, but the precompression required is from 1.5 to 1.6 mm.

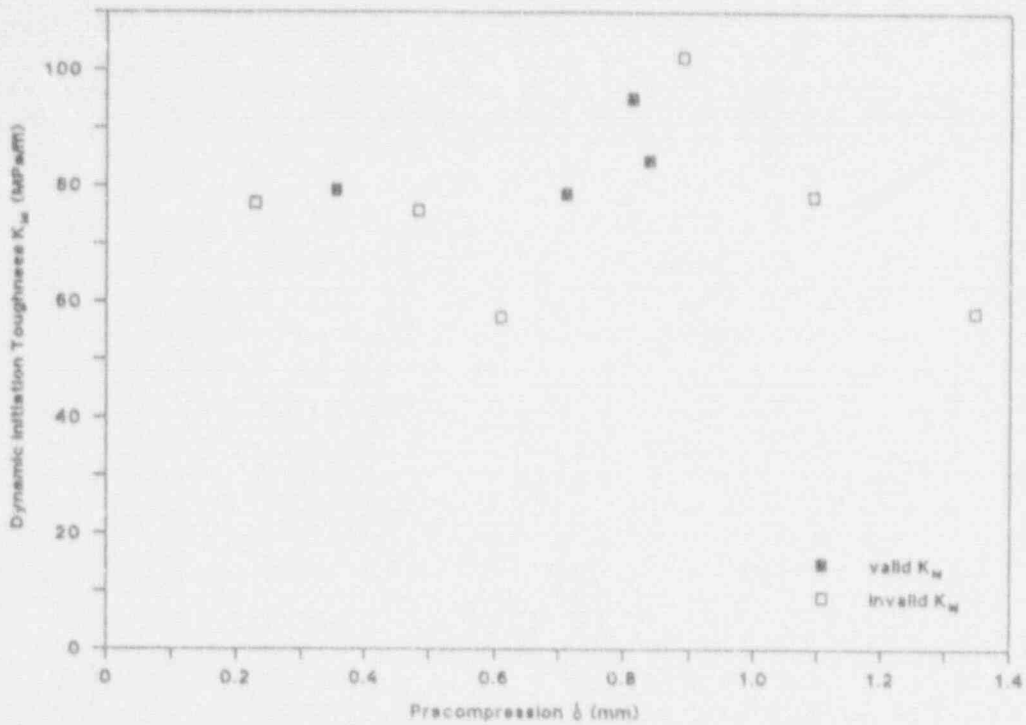

Figure 11 Summary of dynamic initiation toughness K_{Id} as function of amount of precompression δ for T = 20°C (T* = 43°C)

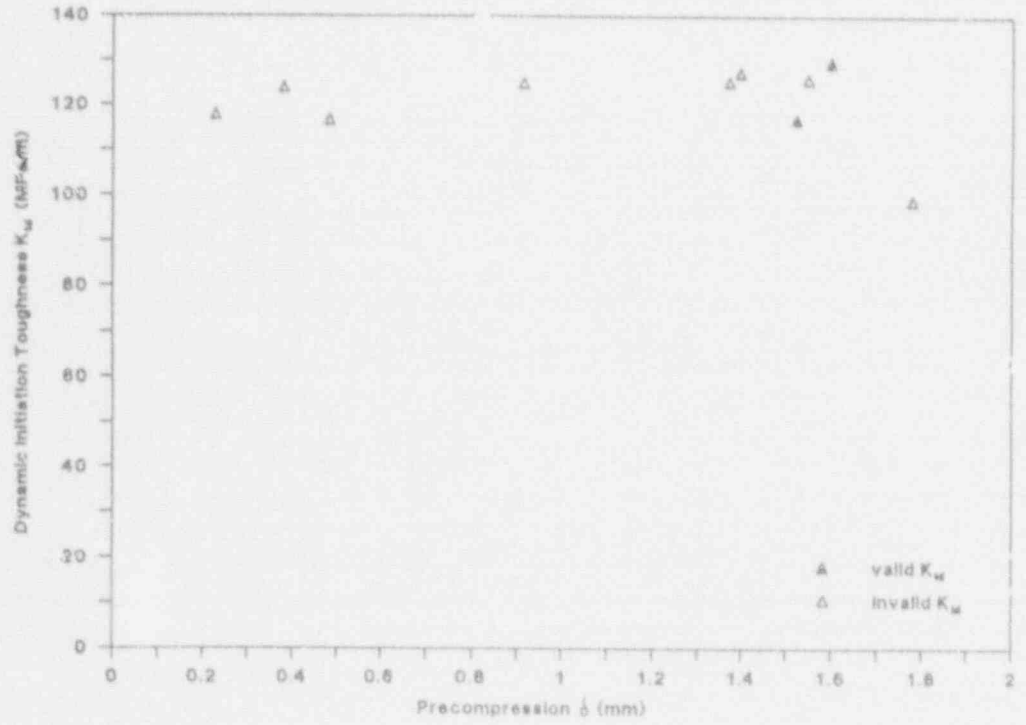

Figure 12 Summary of dynamic initiation toughness K_{Id} as function of amount of precompression δ for T = 42°C (T* = 65°C)

9 Fractographic Analysis

Fractographic analysis is an essential component in the verification that lower-bound values of initiation toughness have been achieved in the notched round-bar test. In determining the lower-bound initiation toughness, one seeks to initiate cleavage with a minimum amount of prior ductile tearing (crack extension by hole formation and then hole joining). It is also important to initiate cleavage from several different sites that are distributed randomly about the circumference of the sharpened notch. Finally, the initiation sites should all be activated at nearly the same time or at the same load. Analysis of the fracture surface in a scanning electron microscope (SEM), with a magnification of about 9×, shows several surface characteristics that verify the adequacy of the lower-bound determination.

An example of the surface features for a fractured round-bar specimen that did not provide a valid lower-bound determination is presented in Fig. 13. The crack extended by hole joining in a ductile tearing mode. The crack extension by ductile tearing varied around the circumference from a minimum of 1.8 mm to a maximum of 3 mm. In this case, the crack extension by tearing occurred at a low velocity (0.5 to 5 m/s) while the specimen remained under dynamic load for more than 600 μs (Fig. 7). The crack extension underwent a transition from ductile to brittle at an initiation site located at point A. The crack then extended at high velocity (≈500 m/s) over the central region of the specimen in a mode that was predominantly cleavage. Even in the central region, ridges are observed, indicating some areas of fibrous failure between cleavage regions.

Next, consider the second example (Fig. 14) that illustrates a valid lower-bound determination. At the outer edge of the fractured area, a ring impression with a uniform thickness is evident, indicating that the axial precompression was performed with controlled alignment. Next, the extension of the crack by ductile hole joining was limited to only 0.3 mm at the crack front in the third quadrant and 5 to 10 μm around the crack front in the first and fourth quadrants. Crack initiation occurred at about ten cleavage initiation sites distributed randomly about the circumference. Most initiation sites were located in regions along the crack front where the ductile tearing was minimized. The crack propagated at high speed (≈500 m/s) across almost the entire test section. The specimen failed in 100 μs, with a strain-time record similar to that shown in Fig. 6. This strain-time trace shows a well-defined peak, with no evidence of the plateau that is evident when extensive ductile tearing occurs.

The final example, presented in Fig. 15, shows a borderline determination of the lower-bound toughness. The test was considered valid, and the data are included in Fig. 9; however, the validity of the test is questionable. The fractograph clearly shows initial crack extension by hole joining, which varied in depth from 0.2 to 0.9 mm. Cleavage was initiated at a limited number of sites, and high-speed crack propagation took place from the bottom portion of the fracture area at site A toward the top of the area. The strain-time traces also showed the effect of crack extension by ductile hole joining because of the low velocity of crack propagation associated with tearing. The time required to fail was ~170 μs, which was long compared with many other valid tests. Also, the strain-time trace shown in Fig. 16 exhibited a plateau duration of ~40 μs; this is indicative of the load relief produced by plastic strain and by low-velocity crack extension of ~1 mm.

The amount of crack extension by ductile hole joining that can be tolerated in a lower-bound determination is still an open issue. It is clear that the tearing relieves constraint and blunts the crack. In some instances, tearing may also elevate the apparent toughness, although the tests at $T^* = 65°C$ seem to indicate that the initiation toughness for tearing and cleavage is about the same. To eliminate possible error, the amount of tearing permissible in a lower-bound determination must be limited. These early results indicate that a ductile crack extension of 0.9 mm may be excessive.

10 Summary

Results for the cleavage initiation toughness for two different heats of A 533 B reactor grade steel are shown in Figs. 9 and 10. In both figures, the temperature T^* is relative to RT_{NDT}, which was –2 and –23°C for heat Nos. 1 and 2, respectively. The results from the notched round-bar tests are compared with toughness determinations made by others using different specimens that were larger in size.

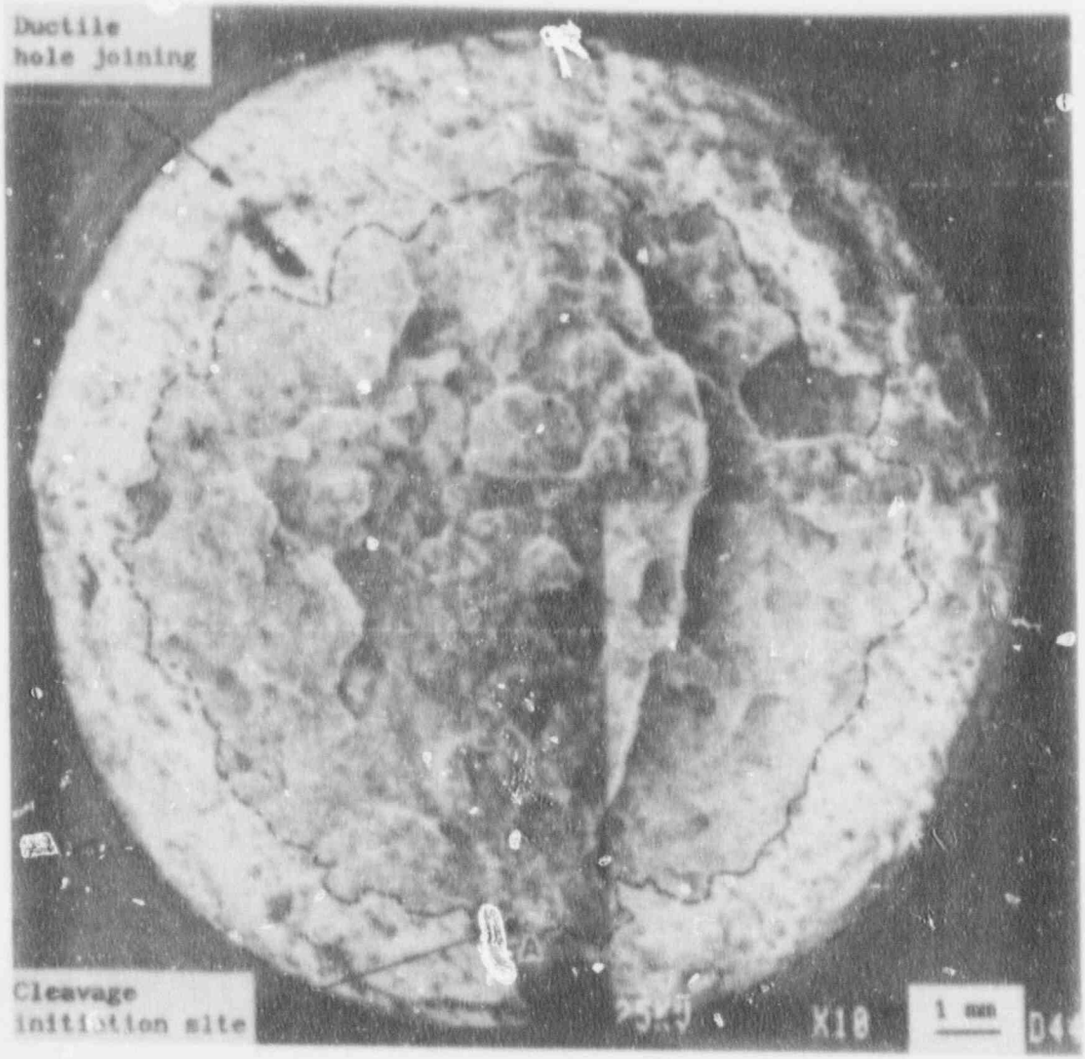

Figure 13 Fracture surface exhibiting extensive ring area where crack extension occurred by hole joining before cleavage initiation

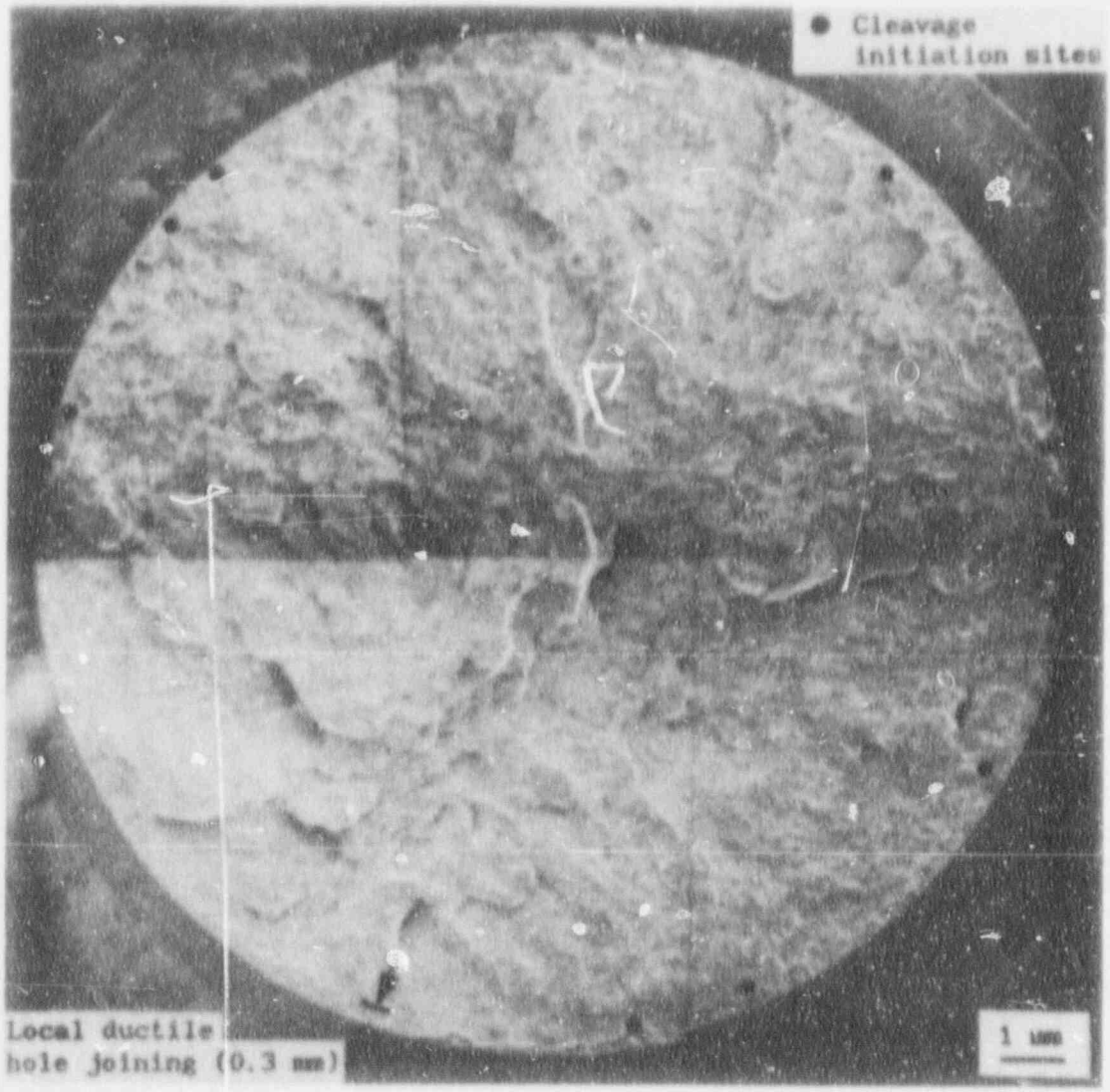

Figure 14 Fracture surface exhibiting very limited hole joining. Initiation is at multiple sites about circumference, and extension is dominated by cleavage

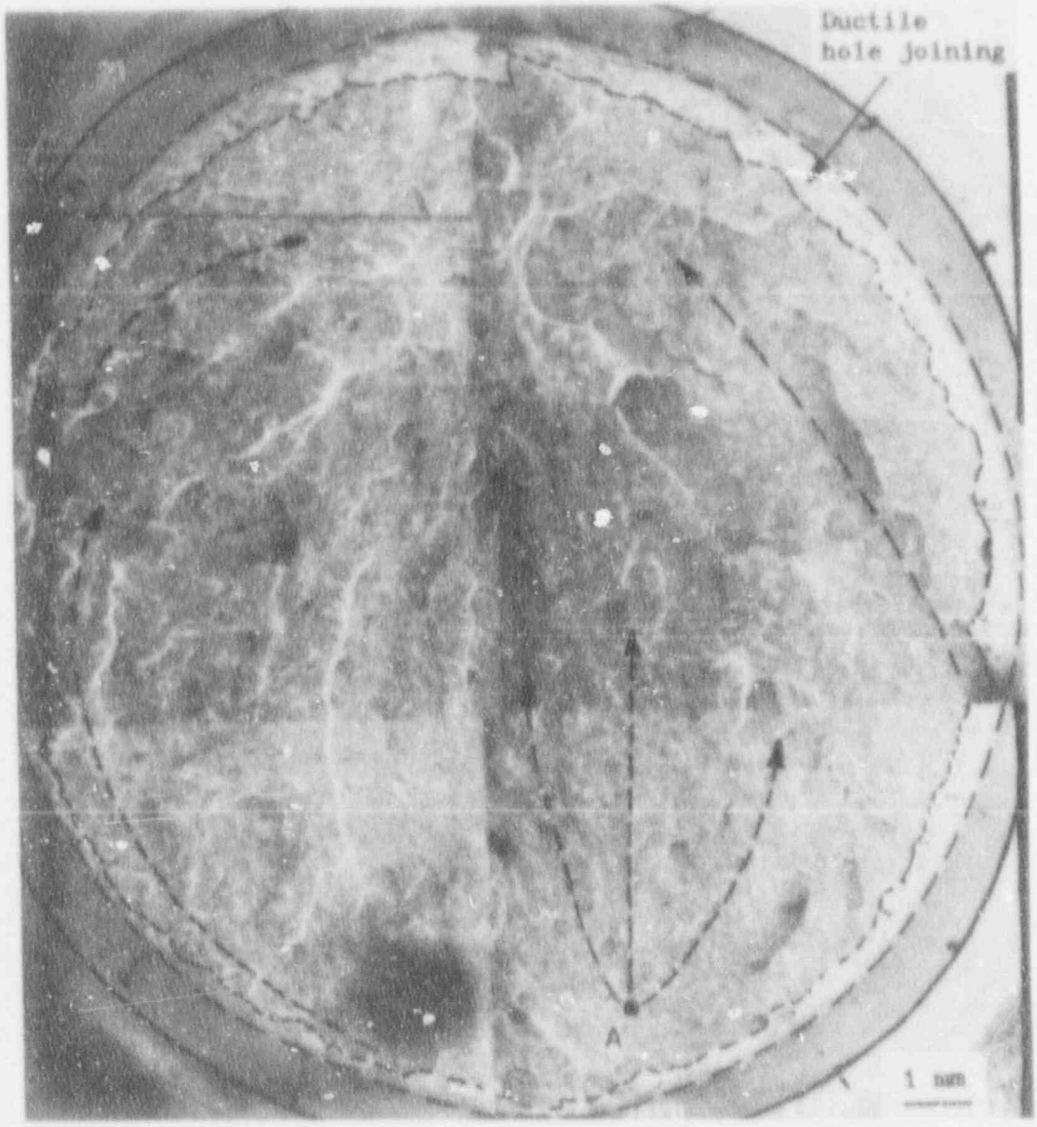

Figure 15 Fracture surface exhibiting moderate amount of crack extension by joining before cleavage initiation from limited number of initiation sites

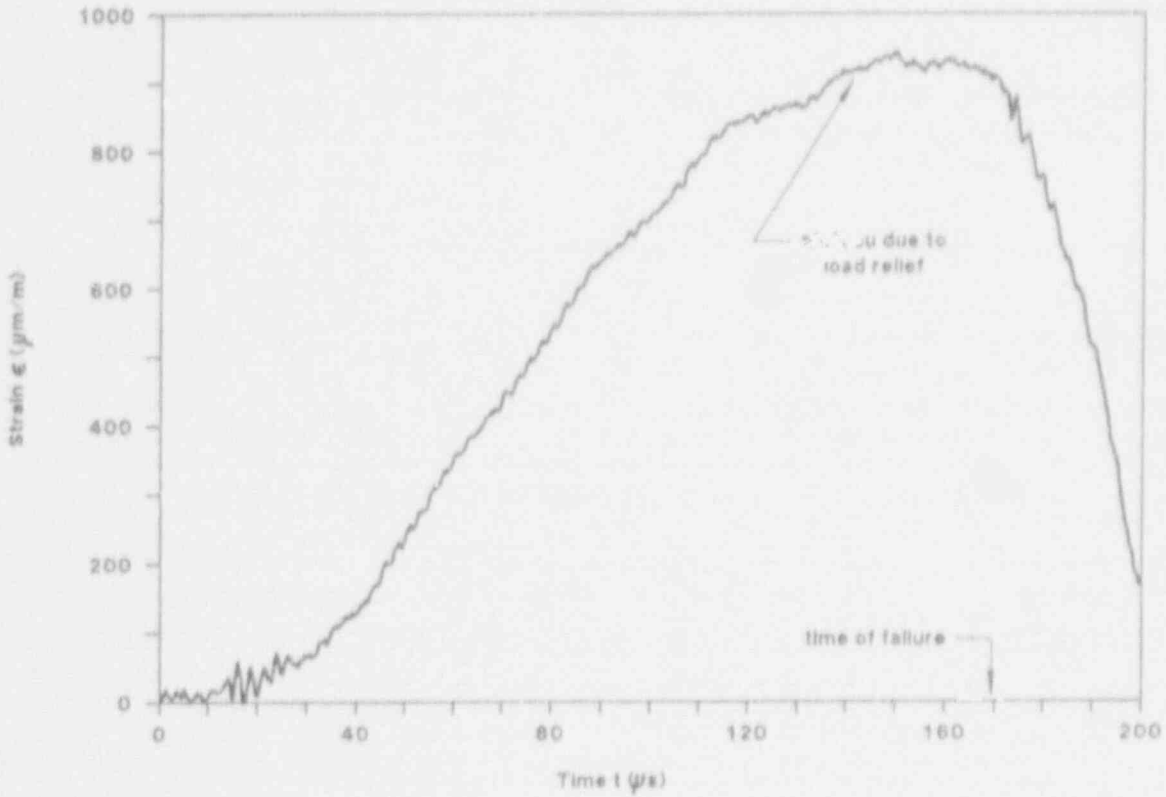

Figure 16 Strain-time trace associated with borderline test (gage-average trace)

These determinations include PTSE-1, ORNL TSE, COOP program, and the Round Robin experiments.

The data from the notched round bar compare favorably with the initiation toughness determined in the other test programs, except for the ORNL TSE, which generally gave higher values. The scatter in the data from the notched round bar was somewhat smaller than the scatter observed in the Round Robin crack-arrest testing.

The amount of precompression required to minimize ductile tearing increases with the temperature T*. For heat No. 1 of A 533 B steel with RT_{NDT} = –2°C, it was observed that the amount of precompression required ranged from 0.4 mm at T* = 5°C to 1.2 mm as T* increased to 52°C. However, it should be noted that the application of this amount of precompression did not ensure cleavage initiation in every test. Instead, the effect of the precompression was to increase the probability of cleavage initiating from several sites with a very small extension of the crack by ductile tearing.

The amount of precompression required for specimens fabricated from heat No. 2 of A 533 B steel, with RT_{NDT} = –23°C, was examined in more detail. At T* = 43°C, cleavage initiation occurred for precompressions ranging from 0.36 to 1.35 mm, although the useful range of precompression is much smaller. The K_{Id} associated with cleavage initiation appeared to depend on the amount of precompression. Specimens with precompressions of 0.7 to 0.9 mm gave valid measures of K_{Id}. Specimens having precompressions <0.7 mm did not reliably initiate cleavage, and specimens with precompressions >0.9 mm initiated cleavage prematurely (i.e., at artificially low stress levels).

As the temperature increased to T* = 65°C, the initiation toughness increased, and the range of precompression required to determine a valid K_{Id} increased to 1.5 to 1.6 mm. In this set of experiments, it was noted that the cleavage initiation toughness and the tearing initiation toughness were about the same.

11 Conclusions

The notched round-bar test procedure provides an inexpensive method to determine lower-bound initiation toughness with relatively small scatter. Measurements of the lower-bound toughness were made with A 533 B reactor-grade steel, a relatively tough material, to a temperature $T^* = 65°C$. The lower-bound toughness varied from 74 to 130 MPa•$\sqrt{m}$ as the temperature T* was increased from 5 to 65°C.

Acknowledgments

The authors would like to thank Claud E. Pugh and William R. Corwin, of Oak Ridge National Laboratory, for providing support and encouragement in monitoring this research program. Thanks are also due to Dr. Donald B. Barker for his assistance in conducting some of the experiments.

References

1. T. Iwadate et al., "An Analysis of Elastic Plastic Fracture Toughness Behavior for J_{1c} Measurements in the Transition Region," *Fracture Resistance Curves and Engineering Applications, ASTM STP 803, Vol. II*, C. F. Shih and J. P. Gudas, Eds., ASTM, Philadelphia, 1983, pp. 531–561.*

2. J. G. Merkle, Martin Marietta Energy Systems, Inc., Oak Ridge Natl. Lab., "An Examination of the Size Effects and Scatter Observed in Small-Specimen Cleavage Fracture Toughness Testing," USNRC Report NUREG/CR-3672 (ORNL/TM-9088), 1984.†

3. J. D. Landes and D. H. Shaffer, "Statistical Characterization of Fracture in the Transition Region," *Fracture Mechanics, ASTM STP 700*, ASTM, Philadelphia, 1980, pp. 368–382.*

4. J. W. Dally, X. J. Zhang, and G. R. Irwin, "Determining Lower Bound Dynamic Initiation Toughness from Notched Round Bars," *Dynamic Fracture Mechanics for the 1990's, PVP—Vol. 160*, H. Homma, D. A. Shockey, and G. Yagawa, Eds., ASME, New York, 1989, pp. 47–54.*

5. C. Mylonas, "Prestrain, Size, and Residual Stresses in Static Brittle-Fracture Initiation," *Welding Journal, Research Supplement* 38(10), 414s–424s (1959).*

6. C. Mylonas, "The Mechanics of Brittle Fracture," *Proceedings, 11th International Congress of Applied Mechanics*, Munich, Germany, 1964, pp. 652–660.

7. C. E. Turner, "A Note on Brittle Fracture Initiation in Mild Steel by Prior Compressive Pre-Strain," *Journal of the Iron and Steel Institute* 197, 131–135 (1961).*

8. G. T. Jones and C. E. Turner, "A Fracture Mechanics Interpretation of Low-Stress Fractures in Precompressed Mild Steel," *Journal of the Iron and Steel Institute* 25(9), 959–965 (1967).*

9. H. Tada, P. Paris, and G. Irwin, Del Research, Hellertown, Pa., *The Stress Analysis of Cracks Handbook*, 1973, p. 27.1.

10. N. Nakamura, C. F. Shih, and L. B. Freund, Brown University, "Elastic-Plastic Analysis of a Dynamically Loaded Circumferential Notched Round Bar," Materials Research Laboratory Report MRL E-152, Providence, R.I., March 1984.

11. L. S. Costin, J. Duffy, and L. B. Freund, "Fracture Initiation in Metals Under Stress Wave Loading Conditions," *Fast Fracture and Crack Arrest, ASTM STP 627*, G. T. Hahn and M. F. Kanninen, Eds., ASTM, Philadelphia, 1977, pp. 301–318.*

12. D. B. Barker et al., "A ... ort on the Round Robin Program Conducted to Evaluate the Proposed ASTM Standard Test Method for Determining the Plane-Strain Crack-Arrest Toughness, K_{Ia}, of Ferritic Materials," USNRC Report NUREG/CR-4996 (ORNL/Sub/79-7778/4), 1988.†

---

*Available in public technical libraries.
†Available for purchase from National Technical Information Service, Springfield, VA 22161.

NUREG/CR-5847
ORNL/Sub/79-7778/8
Dist. Category RF

Internal Distribution

1. D. J. Alexander
2. B. R. Bass
3. J. W. Bryson
4. E. W. Carver
5–6. R. D. Cheverton
7. J. M. Corum
8. W. R. Corwin
9. T. L. Dickson
10. F. M. Haggag
11. J. J. Henry
12. W. F. Jackson
13. J. E. Jones Jr.
14. S. K. Iskander
15. J. Keeney-Walker
16. W. J. McAfee
17. D. E. McCabe
18. J. G. Merkle
19. R. K. Nanstad
20. D. J. Naus
21–25. W. E. Pennell
26. C. B. Oland
27. C. E. Pugh
28. G. C. Robinson
29. D. K. M. Shum
30. R. L. Swain
31–34. T. J. Theiss
35. E. W. Whitfield
36. ORNL Patent Section
37. Central Research Library
38. Document Reference Section
39–40. Laboratory Records
41. Laboratory Records (RC)

External Distribution

42. L. C. Shao, Director, Division of Engineering, U.S. Nuclear Regulatory Commission, Washington, DC 20555
43. C. Z. Serpan, Jr., Division of Engineering, U.S. Nuclear Regulatory Commission, Washington, DC 20555
44. E. M. Hackett, Division of Engineering, U.S. Nuclear Regulatory Commission, Washington, DC 20555
45. A. L. Hiser, Division of Engineering, U.S. Nuclear Regulatory Commission, Washington, DC 20555
46-48. S. N. M. Malik, Division of Engineering, U.S. Nuclear Regulatory Commission, Washington, DC 20555
49. M. E. Mayfield, Division of Engineering, U.S. Nuclear Regulatory Commission, Washington, DC 20555
50. A. Taboada, Division of Engineering, U.S. Nuclear Regulatory Commission, Washington, DC 20555
51–56. J. W. Dally, Department of Mechanical Engineering, University of Maryland, College Park, MD 20742
57. W. L. Fourney, Department of Mechanical Engineering, University of Maryland, College Park, MD 20742
58. J. D. Landes, The University of Tennessee, Knoxville, TN 37996-2030
59. S. T. Rolfe, The University of Kansas, Lawrence, KS 66045-2235
60. A. R. Rosenfield, Battelle Columbus Division, Columbus, OH 43201
61. C. W. Schwartz, Department of Civil Engineering, University of Maryland, College Park, MD 20742
62. E. T. Wessel, 312 Wolverine, Haines City, FL 33844
63. Office of Assistant Manager for Energy Research and Development, DOE–OR, Oak Ridge, TN 37831
64–65. Office of Scientific and Technical Information, P. O. Box 62, Oak Ridge, TN 37831

NRC FORM 335 (2-89) NRCM 1102, 3201, 3202

U.S. NUCLEAR REGULATORY COMMISSION

BIBLIOGRAPHIC DATA SHEET

(See instructions on the reverse)

1. REPORT NUMBER (Assigned by NRC, Add Vol., Supp., Rev., and Addendum Numbers, If any.)
NUREG/CR-5847
ORNL/Sub/79-7778/8

2. TITLE AND SUBTITLE
The Influence of Precompression on the Lower-Bound Initiation Toughness of A 533 B Reactor-Grade Steel

3. DATE REPORT PUBLISHED
MONTH: May
YEAR: 1992

4. FIN OR GRANT NUMBER
B0119

5. AUTHOR(S)
J. W. Dally, G. R. Irwin, X-J. Zhang, R. J. Bonenberger

6. TYPE OF REPORT
Technical

7. PERIOD COVERED (Inclusive Dates)

8. PERFORMING ORGANIZATION – NAME AND ADDRESS (If NRC, provide Division, Office or Region, U.S. Nuclear Regulatory Commission, and mailing address; if contractor, provide name and mailing address.)

Department of Mechanical Engineering
University of Maryland
College Park, MD 20742

Under Contract to:
Oak Ridge National Laboratory
Oak Ridge, TN 37831-6285

9. SPONSORING ORGANIZATION – NAME AND ADDRESS (If NRC, type "Same as above"; if contractor, provide NRC Division, Office or Region, U.S. Nuclear Regulatory Commission, and mailing address.)

Division of Engineering
Office of Nuclear Regulatory Research
U.S. Nuclear Regulatory Commission
Washington, DC 20555

10. SUPPLEMENTARY NOTES

11. ABSTRACT (200 words or less)

This report first describes the test method employing a precompressed round bar subjected to impact loading to initiate a cleavage fracture. The procedure to convert strain measurement into dynamic initiation toughness K_{Id} is described. Also, the results of a fractographic analysis are correlated with the features observed on the strain-time traces, and techniques used to distinguish initiation by either cleavage or ductile tearing are presented.

12. KEY WORDS/DESCRIPTORS (List words or phrases that will assist researchers in locating the report.)

crack arrest
reactor vessel steels
cleavage-fibrous behavior
round-bar specimen

13. AVAILABILITY STATEMENT
Unlimited

14. SECURITY CLASSIFICATION
(This Page)
Unclassified
(This Report)
Unclassified

15. NUMBER OF PAGES

16. PRICE